**International Journal of Mechanical Engineering and Technology (IJMET)**
Volume 10, Issue 01, January 2019, pp. 52–61, Article ID: IJMET_10_01_005
Available online at http://www.iaeme.com/ijmet/issues.asp?JType=IJMET&VType=10&IType=1
ISSN Print: 0976-6340 and ISSN Online: 0976-6359



# PREPARATION OF POROUS CERAMIC MATERIAL FROM WASTE GLASS AND CALCINED KAOLIN USING YEAST AS PORE FORMING AGENT

**Majid M. Shukur, Firas J. Hmood, Shahad J. Jasim**
Department of ceramic & Building Materials Engineering,
University of Babylon, Babil, Hilla, Iraq

**ABSTRACT**

*Production of light-weight porous ceramic media from metakaolin and waste glass powder with sodium silicate as foaming agent in batch1 and without sodium silicate in batch 2 was investigated. Different weight percentages of yeast (0.1-0.5) as pore forming agent have been added to both batches. All samples were formulated by wet milled, dried, shaped and fired at 700°C for batch 1and at 850°C for batch 2. Chemical and mineralogical analysis, identification and calculation of crystalline to amorphous ratio phases by XRD, microstructure and mechanical and physical properties were investigated to specify the resulting porous article. The predominant closed porosity is found in batch 1 whereas open pores are prevalent in batch 2. The size of pores ranges from 3.794mm to 58µm in batch No. 1 and from 67.5 µm to 1.6 µm in batch No. 2 (millimeter to sub-micron) with approximately spherical shape were found in both batches.*

**Key words:** porous ceramic, metakaolin, waste glass, pore forming agent.

**Cite this Article:** Majid M. Shukur, Firas J. Hmood, Shahad J. Jasim, Preparation of Porous Ceramic Material from Waste Glass and Calcined Kaolin Using Yeast as Pore Forming Agent, *International Journal of Mechanical Engineering and Technology* 10(1), 2019, pp. 52–61.
http://www.iaeme.com/IJMET/issues.asp?JType=IJMET&VType=10&IType=1

## 1. INTRODUCTION

Porous ceramic materials have a wide range of industrial applications such as in water and waste water treatment, aeration systems, vibration hiding, compressed gas systems, heat insulation, electronics, sound absorption, food and beverage productions, and fluid filtration [1, 2].

The ceramic pore structures and expected their permeability are considered the key for any technical production route of porous ceramics, materials where goodness quality and accuracy are the major requirement [3]. The most popular materials which are used in production of ceramic porous materials are composed of aluminosilicate particles bonded by

glass and contain different percentage of alumina, which in turn plays an important role in physical and mechanical properties of the final product. Porous ceramic materials may act as a filtration media or as insulation materials. This diversity in its function depends basically upon the geometry and the type of pores structures [4]. Generally, porous ceramic materials have relatively high structural rigidity and low density. In this article, the porous ceramic body was made from locally available Iraqi kaolin which is later converted to network of amorphous aluminosilicate particles. Window glass powder was used to bind these particles and sodium silicate as a foaming factor. In addition, yeast powder was introduced to the batch as a pore forming agent. The prepared porous ceramic material was characterized by x-ray diffraction (XRD), scanning electron microscopy (SEM), and physical properties to know the shape, volume, and pore distribution and finally its structural function.

## 2. EXPERIMENTAL

### 2.1. Starting Materials and samples forming

The prepared porous ceramic where is mainly consisting of aluminosilicate powder as metakaolin, window glass powder, sodium silicate, and backing yeast as pore forming agent. The principal batches are formulated on the basis of own previous study [5]. In which different compositions of the above-mentioned components were tested. The recipe of 20 wt% metakaolin, 40 wt% window glass powder and 40 wt% sodium silicate was chosen as a best batch in accordance with the physical and mechanical results. Table 1 shows the two batches which are adopted in the current study. Metakaolin component was obtained by dihydroxylation process of Iraqi kaolin clay at a temperature of 582 °C for 1.5 h. The glass powder was soda-lime glass waste and hydrated sodium silicate ($Na_2SiO_3.5H_2O$) was used as foaming agent. Commercial baker's dry yeast is included in the batch recipes as pore forming agent.

**Table 1** Composition recipe of the batches.

| Batch No. | Metakaolin % | Glass powder % | Sodium silicate % | Yeast % |
|---|---|---|---|---|
| 1 | 20 | 40 | 40 | 0, 0.1, 0.2, 0.3, 0.4, 0.5 |
| 2 | 33.5 | 66.5 | - | 0, 0.1, 0.2, 0.3, 0.4, 0.5 |

All batches components are milled by a ball mill (SFM-1, QM-3SP2) to very fine powder for 24 h and sieved by a sieve of 200 mesh. The batch powders were wet mixed and milled with ethanol in a planetary ball mill for 6 h and then dried in an oven at 50 °C. Cylindrical samples with dimensions of 20x10 mm were prepared via biaxial pressing method using a pressing machine (CT340-CT440) at 100 MPa. The samples of the first batch were sintered at a temperature of 700 °C, while the second batch samples were sintered at 850 °C.

### 2.2. Characterizations

Calcination temperature of Iraqi kaolin was detected using a differential scanning calorimetry (DSC131, evo, Setaram, France). Metakaolin and waste glass were chemically analyzed by the gravimetric wet method. This analysis was carried out via the Iraqi geological and mining survey. The main oxides of the starting materials were declared in terms of their weight percentages (Table 2). The crystalline phases of the starting materials were identified by the X-ray diffraction (XRD) method (Shimatzu 6000 diffractometer, Japan). Cukα X-ray as a source radiation was used with 40 kV and 30 mA at a scanning speed of 5°/min. Nickel was

used as a filter. The diffraction data were recorded in the range of 2θ = 5-50°.Scanning electron microscopy (SEM FEI, FP 2017/12 inspect S50, Czech Republic)is employed to evaluate the microstructure of the sintered samples. The samples were vertically cut in the c-direction and the fracture surfaces were etched with 2% HF acid for 10 s. The surfaces were coated with gold by a plasma sputter (Quorum Q150 R ES) to prevent charging accumulated on the sample surface which causes image distortions.

The density and porosity measurements were measured after the Archimedes principle and calculated according to ASTM 373-88. While the compressive strength was measured using an instrument (WDW-5E) with a cross head speed of 1 mm/min. The physical, mechanical, and thermal properties were measured as an average of three-time measurements.

### 2.3. Calculation of phase amounts in the sintered samples

An attempt was done to calculate the amorphous and the crystalline phase percentages in the two batches utilizing the X-ray patterns of the sintered samples in conjunction with XPert High Score Plus software. In this method, 20 wt% of $LaB_6$ was added to each sample and quantitatively analyzed. The starting structures models for the detected phases were obtained from Inorganic Crystal Structure Database (ICSD). The structure numbers of quartz (27745), nepheline (85553), cristobalite (24587) and lanthanum hexaboron (40947) which was used as an internal standard were adopted in the quantitative analysis.

The Rietveled method was used to quantify the crystalline and amorphous contents according to experimental techniques found elsewhere in reference [6]. Samples of particle size less than 45 μm were used for this purpose. The refinement cycle consisted of global parameters like overall zero shift, specimen displacement, background, scale factors at the beginning, and then cell parameters which have done carefully. After several refinement cycles, if the agreement indices like weighted-R percent (Rwp) and goodness of fit (GoF) are less than 12 and 5 respectively, the results are accepted.

## 3. RESULTS AND DISCUSSION

### 3.1. Thermal analysis

Dehydration temperature of the starting kaolin was determined by the DSC. Figure 1 illustrates an endothermic peak which was assigned for the kaolin dehydration reaction. The peak temperature is 582 °C. Therefore, the starting kaolin was heat treated at this temperature for an hour to turn it to metakaolin.

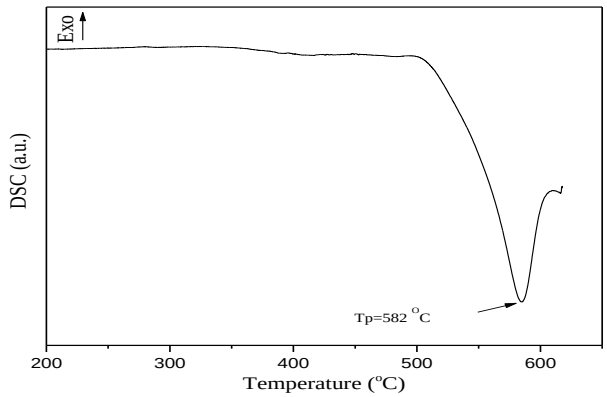


**Figure 1**. DSC analysis of Iraqi kaolin

## 3.2. Chemical and mineralogical analysis of starting materials

Table 2 lists the chemical and mineralogical analysis of the starting materials according to normative minerals calculations (Norm). The kaolinite and quartz minerals appear as the dominant phases present in the Iraqi kaolin deposits. The calcination process of the kaolin at 582 °C allows to form an amorphous metakaolin new phase on expense of the kaolinite mineral. It appears that 80 % of kaolinite mineral in the kaolin ore was dropped to 18.8 % via a calcination process and 61.2 % of mtakaolinite was present as an alternative structure.

**Table 2.** Chemical and mineralogical analysis of starting materials.

| Oxide % | Kaolin | Kaolin after calcination | Glass powder |
|---|---|---|---|
| $SiO_2$ | 51.07 | 56.07 | 68.8 |
| $Al_2O_3$ | 31.67 | 35.7 | 1.23 |
| $TiO_2$ | 1.26 | 1.48 | 0.06 |
| $Fe_2O_3$ | 1.37 | 1.56 | 0.42 |
| MgO | 0.09 | 0.11 | - |
| CaO | 1.37 | 1.60 | 9.32 |
| $Na_2O$ | 0.13 | 0.15 | 11.00 |
| $K_2O$ | 0.43 | 0.50 | 0.25 |
| L.O.I | 12.32 | 2.64 | 1.07 |
| Minerals content % | Kaolinite = 80<br>Quartz = 14 | Kaolinite = 18.8<br>Quartz = 14<br>Meta-Kaolinite = 61.2 | |

Quartz mineral is considered a very stable mineral specially at low temperatures, so its content in the kaolin ore does not change after the heat treatment. Hence, the amorphous aluminosilicate structure of metakaolinite grains and the little percentage of kaolin will join by glass powder and form the final starting materials for the next firing process.

## 3.3. X-ray diffraction analysis

Figure 2 illustrates the difference in phase diffraction patterns of kaolin before and after calcination. It is clear that the structure of the starting kaolin has been changed where the main peaks of kaolinite disappeared after calcination. The Figure also indicates that the calcined kaolin retained quartz phase in the disordered matrix of kaolinite.

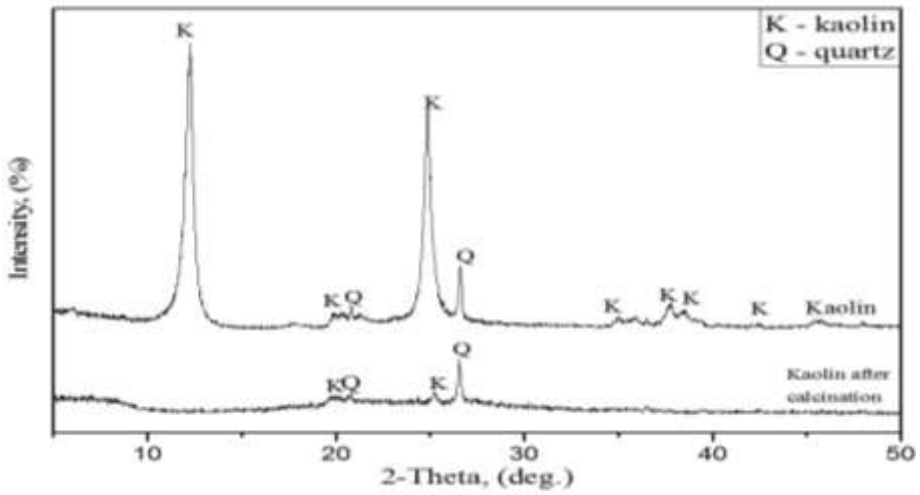


**Figure 2.** XRD patterns of Iraqi kaolin (A) and metakaolin (B) at 582°C. k=kaolinite, Q=quartz.

Figure 3 demonstrates the X-ray patterns of the samples fired at 700 °C for batch No.1 (Figure 3A) and those were sintered at 850 °C for batch No. 2 (Figure 3B). Both batches reveal approximately similar diffractions which represent an amorphous matrix as a broad hump. Besides, there are peaks within these humps indicate existing of crystalline phases grown within it. The crystalline phases are sodium aluminum silicate ($AlNaO_6Si_2$) as nepheline $(Na,K)AlSiO_4$) and silica ($SiO_2$). The silica phase appears as quartz mineral in batch No.1, while arises as quartz and cristobalite in batch No. 2. The quartz mineral is originally attendant in the kaolin starting material which has not affected and structurally changed during the firing process. Hence, the main difference between the two batches is existing of cristobalite phase which is chemically and thermally ready to be grown only in batch No. 2.

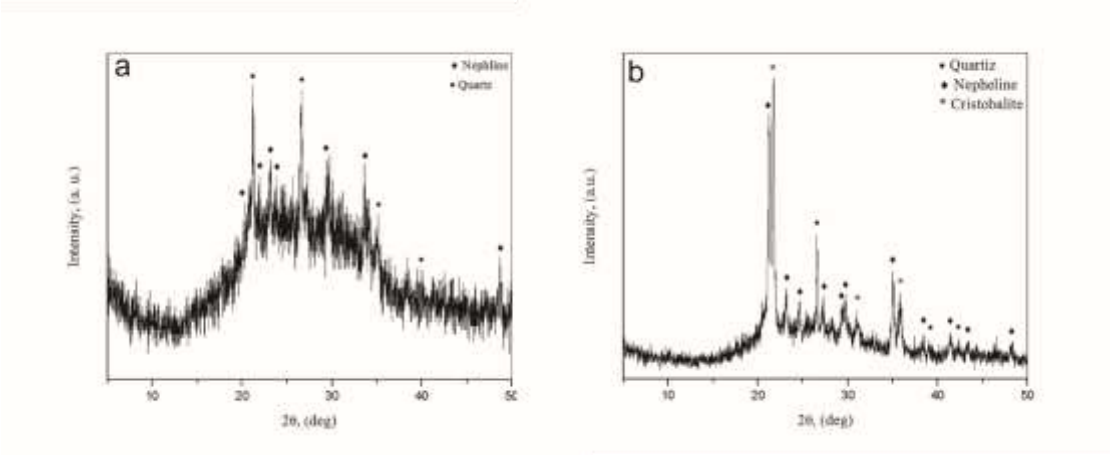


**Figure 3.** X- ray patterns of batch no.1 (A) and batch no. 2 (B).

Table 3 reports the content percentage of both amorphous and crystalline phases for batches No.1 and batch No.2.The agreement indices (Rwp and GOF) that are obtained for batch No.1 are in the acceptable range with values of 18.7 and 1.59 respectively. While the values of 20.5 and 1.8 are recorded for the batch No.2. It may be noticed that the experimental values of Rwp and GOF are somewhat out of their requirement in the analysis, since very slow scan speed was not available at thein X-ray machine.

**Table 3.** Amorphous and crystalline phases of the batches and their ratio for different yeast additives. C = crystalline, A = amorphous.

| Batch NO. | Yeast % | Amorphous | Crystalline phases | | | C/A |
|---|---|---|---|---|---|---|
| | | | Nepheline | Quartz | Cristobalite | |
| 1 | 0 | 65.0 | 26.0 | 9.0 | - | 0.54 |
| | 0.3 | 33.5 | 58.0 | 8.5 | - | 2.0 |
| | 0.5 | 54.3 | 37.0 | 8.7 | - | 0.84 |
| 2 | 0.3 | 33.0 | 33.9 | 9.1 | 24.0 | 2.0 |
| | 0.5 | 23.0 | 42.5 | 8.5 | 26.0 | 3.3 |

It is interesting to know that the base glass composition, nucleating agents and heat treatment are considered the principal factors affecting up on the crystallization of a certain melt [7,8,9]. Quartz phase appears as a constant phase within the crystalline phases and its content doesn't change in the two batches as it imports from the kaolin starting material. Only nepheline and cristobalite were varied in their content. The crystalline to amorphous ratio was

increased up to value of 2 and then dropped to less than 1 with increasing the yeast additive in samples of batch No.1. While samples of batch No.2 show continuously increasing in C/A ratio with more percentage of yeast added. This variation of C/A ratio in both batches may be concluded that the samples of batch No.2 have more network formers and heat treatment energy than that found in samples batch No.1.

## 3.4. Physical properties

### *3.4.1. Porosity*

Figure (4) shows the porosity results including apparent, closed and true porosities as a function of different additive of yeast pore forming agent for batches No. 1 and batch No. 2. First of all, batch No.1 has sodium silicate in its composition recipe, whereas batch No.2 hasn't. When hydrated sodium silicate was existing with the glass powder during the sintering process, chemically bonded ~~of~~ water molecules in the sodium silicate structure commence to be released at temperature range 600-620 °C [10]. The glass transition ($T_g$) of soda-lime glass is around 530 - 570 °C [11,12], which is slightly lower than the foaming action temperature of the sodium silicate. The glass particles start to soften and a liquid phase of this glass will hamper releasing the water molecules in gaseous phase when the sintering temperature reaches up to 620 °C. This mechanism will create a remarkable closed porosity content for batch No.1 in comparison with that found in batch No.2 (Figure 4a). Besides, 10 % of yeast additive as a pore forming agent gives the best result of closed porosity in both batches, where 74 % was found in batch No.1 incompar is on with 33 % in batch No.2. Generally, increasing of yeast content will be creating more open pores in the sample and this result was clearly shown in Figure 4b. True porosity represents subtotal of open and closed porosities. Figure 4c exhibits two different relationships of true porosity as a function of raising additive yeast content in both batches.

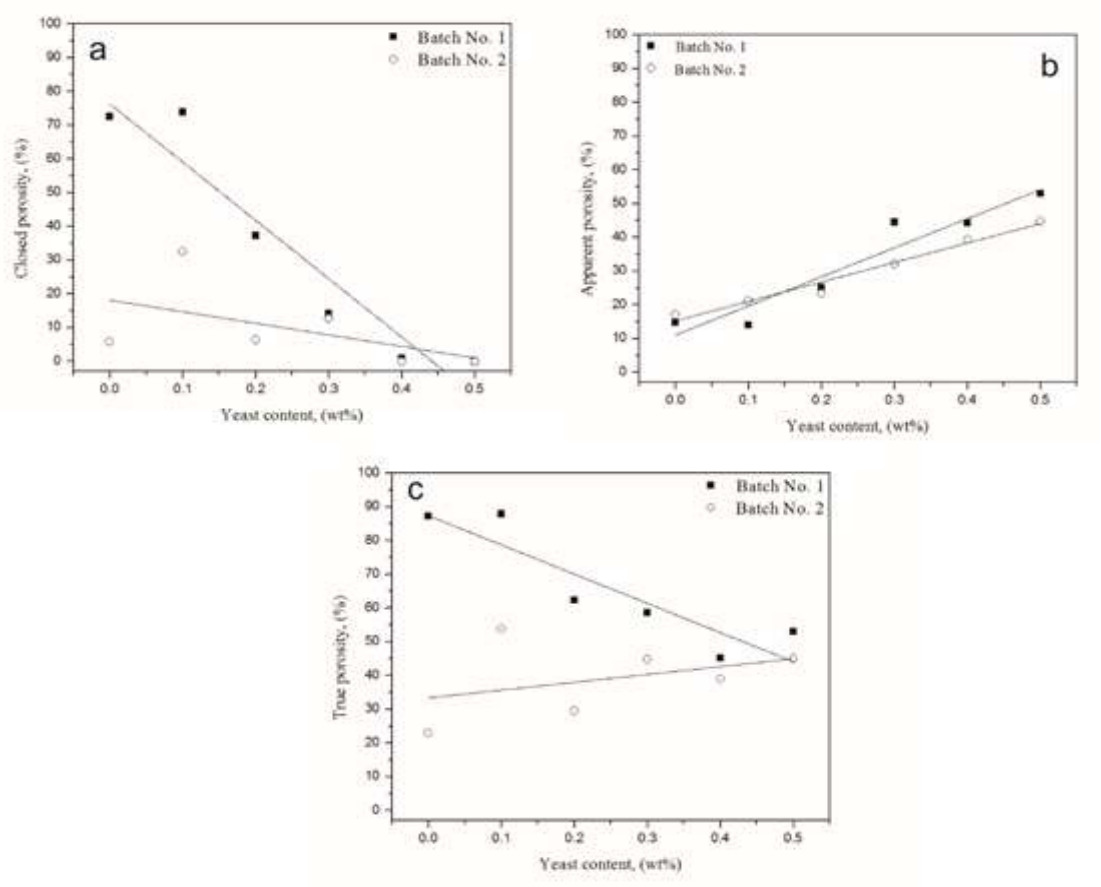


**Figure 4.** Porosities vs yeast percent addition for the batches. (A) closed porosity, (B) apparent porosity, (C) true porosity.

It is found that the values of true porosity in batch No.1 decreased with increasing the percentage content of the yeast, while the opposite behavior has been seen in batch No.2. This behavior may indicate that the presence of sodium silicate as a foaming agent in batch No.1 was played the major role in developing the voids in the sample. On the other hand, the pores in batch No.2 were mainly growing by the action of yeast pore forming agent.

### *3.4.2. Density*

Bulk density of the batches No. 1 and batch No. 2 are depicted with respect to the yeast content percent in the sample (Figure 5). It is observed that the densities of batch No.1 are lower than 1g/cm$^3$, which is in turn, lower than the corresponding of batch No.2 where they show values larger than 1 g/cm$^3$. This decrease in densities of the samples batch No.1 may be attributed to high fraction of true porosity in comparison with the samples of batch No.2.

Usually, the density of the crystal is depended upon both atomic weight of chemical composition and their atomic structure. In this case the two batches have approximately the same chemical composition (metakaolin and soda-lime glass) and the crystal structure. Hence, the microstructure of the sample will be the controller of the density of the sample. Commonly, there is a reverse relationship between the density and porosity of samples formed from one material. According to this fact, the results of bulk density for both batches reveal the opposite behavior with respect of porosity data.

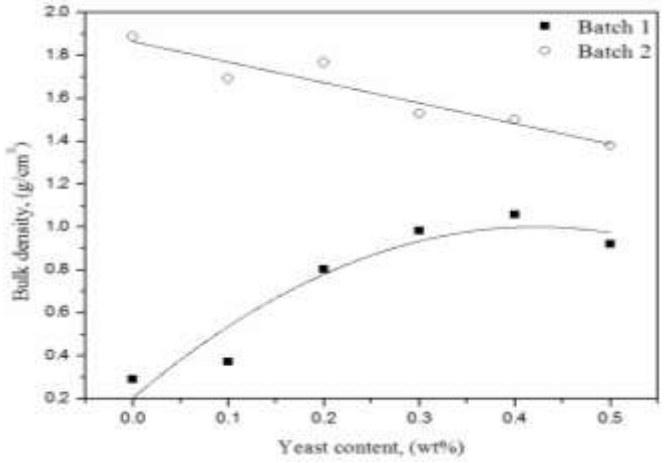


**Figure 5.** Bulk density of batches 1 and 2 at sintering temperatures of 700 and 800 °C respectively.

## 3.5. Mechanical properties

### *3.5.1. Compressive strength*

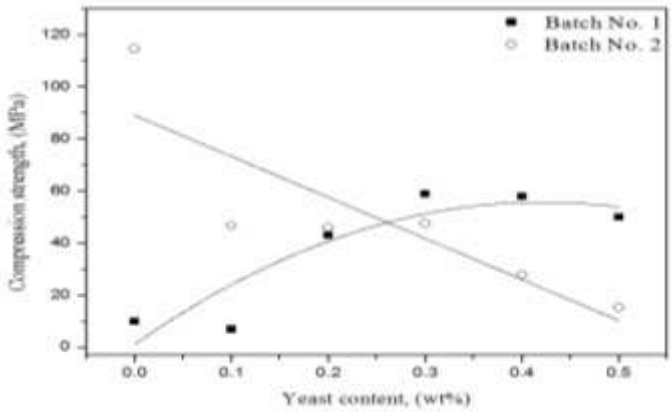


**Figure 6.** Compressive strength of the batches.

The compressive strength of the samples for the two batches, which sintered at different temperatures, depends upon the yeast additions as shown in Figure 6.

Figure (6) depicts the relation between the measured compressive strength in MPa and the yeast content up to 0.5 wt%. The Figure appears two different mechanical behaviors. The compressive strength of batch No. 1 increases with the yeast content up to 0.3 wt% and then decreases for higher contents. While batch No. 2 shows another behavior, in which the compressive strength decreases with increasing the yeast content up to 0.5 wt%. This difference in the two trends can be cleared according to the porosity population results and came agreeably with it. It is well-known that the compressive strength and porosity content of the sample are inversely related.

## 3.6. Microstructure

Figure 7 shows the SEM images of vertical broken surfaces of sintered samples. Image (a) for batch No. 1 with yeast /powder(y/p) ratio of 0.1 shows that the shape of the pores is similar to the spherical shape because the sodium silicate tends to decompose and generate a balanced pressure on the walls surrounding, so the constant pressure gives the form of almost sphere. Obvious differences are found in the morphology with different addition of yeast content.

When (y/p) ratio reach to 0.5 (Figure7b) the yeast particles made small channels that connect the large pores together and made it small and open.

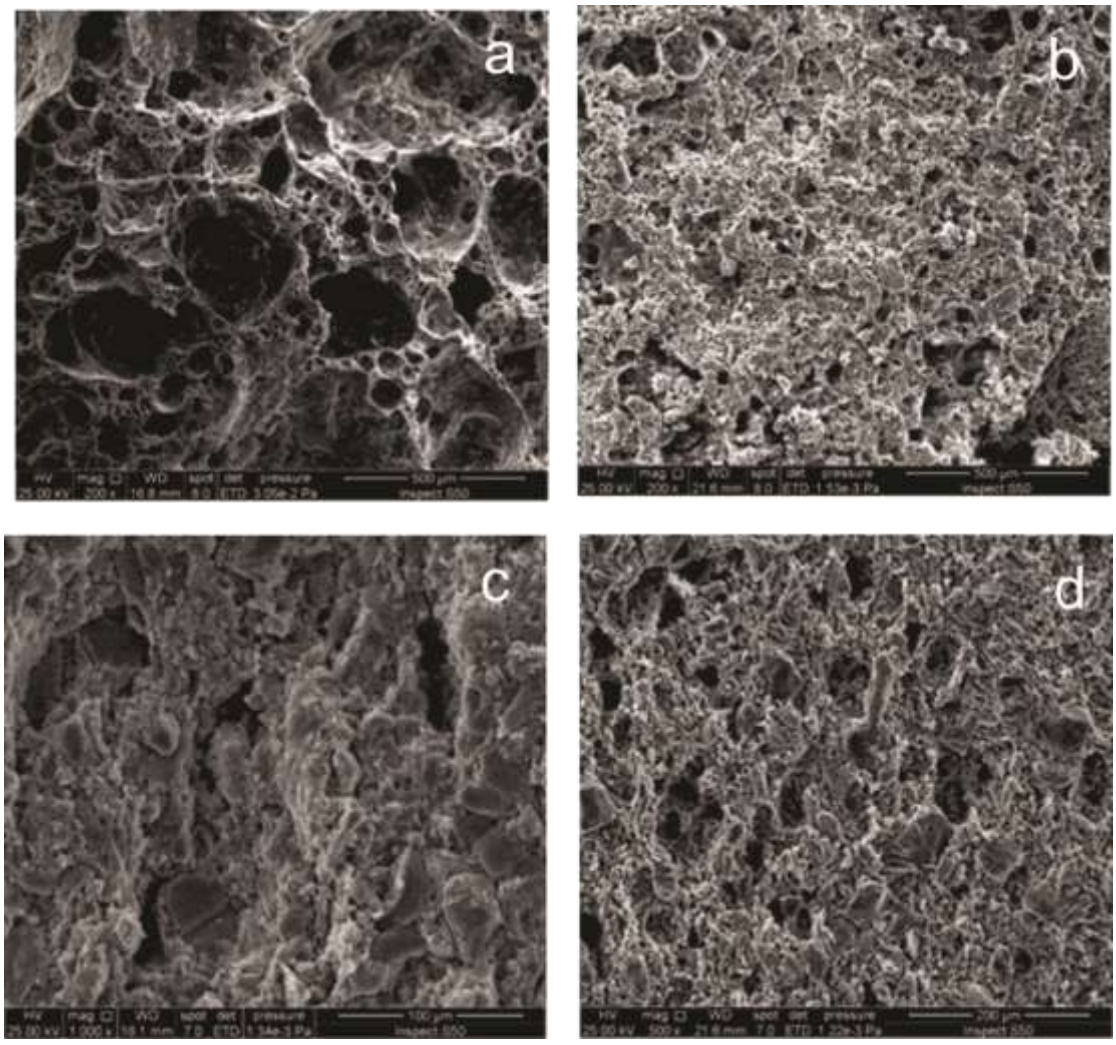


**Figure 7.** SEM micrographs of batch 1(a) 0.1 wt.% yeast (b) 0.5 wt.% yeast and batch 2 (c) 0.1 wt.% yeast (d) 0.5 wt.% yeast.

The SEM micrographs in Figure 7c, which is for batch No. 2 with (y/p) ratio 0.1, shows a good compact with low porosity.This is because the small amount of yeast added; in addition tothe absence of sodium silicate foaming action. Image 7d is for the same batch with a (y/p) ratio of 0.5. Itshows that the shape of pores is identical to that of yeast particles. These images in Figures 7a – 7d show microcracks developed inside the crystals growing from the glassy melt. When these crystals grow as a function of temperature, the microcracks increase and run into the glassy phase.

## 4. CONCLUSIONS

The following conclusions agree with this study objectives which were discussed previously in the introduction:

- The converted kaolin at 582°C (metakaolin) and soda lime glass were successfully used to produce very light-weight ceramic porous media with the help of sodium silicate as a foaming agent and different percentage of yeast additions.

- The resulting porous ceramic ware was a solid framework consist mainly of: quartz, nepheline and cristobalite crystalline phases immersed in a glassy matrix, and voids fraction ranging in size from millimeter to sub-micron.
- The presence of sodium silicate in the samples of batch No.1 was responsible of acquiring the ware high percentage of closed porosity (74 %). While 10 % of yeast addition gives an optimum result of true porosity up-close to 88 %.
- The absence of sodium silicate in the samples of batch No.2 and the action of yeast additions instead of it enhances the growing of open pores on expense of closed pores and this will be continuously increased with raising the yeast percentage additions.
- The cooperation of sodium silicate and yeast additions create approximately spherical shape of pores.
- The physical and mechanical properties are in in agreement with the volume fraction of the formed pores.

# REFERENCES

[1] P.S. Liu, G.F. Chen “Porous Materials processing and applications”,2014; p.576.

[2] Liu P.S., Lang K.M. "Functional materials of porous metals made by P/M, electroplating and some other techniques" J. Material Science. 2000; 36 (21): 5059-5072.

[3] Nakajima H. "Fabrication, properties and applications of porous metals with directional pores" Proc. Jpn. Acad B. Phys Bio Sci, 2010; 86(9): 884-899.

[4] Ouyang D.G., Jiang Y.H., Wang HQ, Luo W, Zhu SH, Li MH." Development of honeycomb ceramics thermal storage with low stress." Indus. Fum. 2009; 31(5): 8-10.

[5] Majid M.S., Ammar T.K., "Characterization of ceramic foam from metakaolin and waste glass by sodium silicate agent "International Conference on Advance of Sustainable Engineering and its Application (ICASEA), IEEE Publisher; 2018.

[6] Nestor U.A., Haci B., Andres R., Mauricio H.C., Jose L.V., "An investigation of the effect of migratory type corrosion inhibitor on mechanical properties of zeolite-based novel geopolymers" J. of Molecular Structure journal, 2017; 1146, p.814-820.

[7] Holand W., Beall G. "Glass ceramic technology." The American Ceramic Society; 2002.

[8] Ray C.S., Fang X., Day D.E.,"New method for determining the nucleation and crystal-growth rates in glasses",J. Am.Cera. Soc., 2000; 83, p.865-872.

[9] Galina A. S., “Crystal Growth and Nucleation in Glasses in the Lithium Silicate System”, J. of Crystallization Process and Technology, 2016; 6, p.29-55

[10] Djobo J.N.Y., Tchadjie L.N., Tchaloute H.K., Kenne B.B.D., Elimbi A., Njopwouo D."Synthesis of geopolymer composites from a mixture of volcanic scoria and metakaolin" J. Asian Ceramic Society; 2014, NO.12.

[11] Kadhim Naief Kadhim and Ghufran A. (The Geotechnical Maps For Gypsum By Using Gis For Najaf City (Najaf - Iraq) (IJCIET), Volume 7, Issue 44, July-August 2016.

[12] Eric L.B." Glass mechanical and technology." Wiely-VCH; 2008, P.366.